American Journal of Mathematical and Computer Modelling
2026, Vol. 11, No. 2, pp. 81–97
https://doi.org/10.11648/j.ajmcm.20261102.11

Research Article

A Mathematical Model of *Helicobacter pylori* Transmission Incorporating Antibiotic Resistance

Vincent Kyunguti Mwanthi[1, *], Stephen Karanja[1], Loyford Njagi[1], Mark Kimathi[2]

[1]Department of Mathematics, Meru University of Science and Technology, Meru, Kenya
[2]Department of Mathematics and Statistics, Machakos University, Machakos, Kenya

Abstract

Helicobacter pylori (*H. pylori*) infection remains a major public health concern, particularly in developing countries with inadequate sanitation. The increasing rate of antibiotic resistance complicates treatment, prolongs infections, increases household transmission, and raises the risk of complications like stomach ulcers, highlighting the need for improved interventions. This study develops and analyzes a mathematical model of *H. pylori* transmission that incorporates antibiotic resistance, classifying infectious individuals into drug-sensitive, drug-resistant, and stomach ulcer cases. Individuals with drug-sensitive infections are treated with *first-line* antibiotics, those with drug-resistant infections are treated with *second-line* antibiotic therapy, and patients infected with stomach ulcer cases undergo specialized antibiotic management. Moreover, the transition from drug-resistant to drug-sensitive cases occurs as treatment suppresses resistant strains, letting sensitive strains dominate. Analytical results show that the basic reproduction number $\Re_c$; is the sum of two reproduction numbers $\Re_s$ and $\Re_r$ representing the contribution of the sensitive and resistant strains, respectively. The disease-free equilibrium is locally asymptotically stable when $\Re_c<1$, indicating possible eradication under effective control measures, while the endemic equilibrium is stable when $\Re_c>1$, implying persistent transmission. Sensitivity analysis identifies critical parameters that influence the persistence of *H. pylori* in the population. Numerical simulations demonstrate that improved hygiene and sanitation, together with the use of appropriate and timely antibiotic therapy, significantly reduce the prevalence of sensitive and resistant strains, limit stomach ulcer development, and lower the overall infection burden.

Keywords

Helicobacter Pylori, Drug-sensitive Strain, Drug-Resistant Strain, Antibiotic Resistance, Reproduction Number, Numerical Simulation

1. Introduction

Helicobacter pylori (*H. pylori*) is a globally prevalent pathogen associated with chronic gastritis, peptic ulcer disease, and gastric cancer [1]. The growing emergence of antibiotic-resistant strains, particularly resistance to clarithromycin and metronidazole, has become a major clinical and public health concern [2]. This resistance reduces the effectiveness of standard eradication regimens and contributes to persistent and re-

*Correspondence: Vincent Kyunguti Mwanthi (mwanthiv@gmail.com)

Received: 19 March 2026; **Accepted:** 30 March 2026; **Published:** 24 April 2026

current infections. Resistance mechanisms include point mutations in rRNA genes, efflux pump activation, and biofilm formation, all of which affect bacterial fitness and transmission dynamics [5]. Understanding these dynamics is critical for developing effective intervention strategies and optimizing antibiotic use [6].

H. pylori is commonly transmitted from an infected individual to a susceptible person through direct person-to-person contact, primarily via oral-to-oral and fecal-to-oral routes. This includes close interactions such as kissing, exposure to vomitus, oral sexual contact, and possibly breastfeeding. Additionally, the pathogen may be spread indirectly through environmental sources, particularly through the consumption of contaminated food or water [8, 9].

Smit et al. [3] on their study on infections with *H. pylori* and challenges encountered in Africa. Highlighted that globally, Africa carries the highest burden of *H. pylori* infection, with an estimated prevalence of 70.1%, followed by South America (69.4%) and Western Asia (66.6%). The high prevalence in Africa is largely attributed to socioeconomic factors such as poor sanitation, overcrowding, and limited access to healthcare, which are common in many developing countries [7]. In Kenya, Smith et al. [3] highlighted that infection rates are higher among children (73.3%) than adults (54.8%), indicating early-life acquisition and sustained transmission. These findings highlight the importance of implementing targeted *H. pylori* prevention and control strategies [4].

An increasing number of scholars have endorsed the "Kyoto Global Consensus Report on *H. pylori* Gastritis reclassifying *H. pylori* gastritis as an infectious disease, reinforcing the need for systematic detection and eradication to prevent ulcer disease and gastric cancer [14]. The more recent and up-to-date "Maastricht VI/Florence Consensus Report" provides updated international guidance, recommending treatment of all confirmed infections unless contraindicated and emphasizing strategies to address antibiotic resistance [11].

In Kenya, standard treatment combines acid suppressants, antibiotics, and bismuth agents [12]. However, increasing antibiotic resistance has reduced eradication rates and increased treatment failures [8, 10]. Repeated empirical therapy and irregular drug use in primary care exacerbate resistance, further complicating eradication. Despite recent refinements in treatment strategies, cure rates have not shown substantial improvement [13].

Mathematical modeling has been increasingly applied to study *H. pylori* transmission and infection dynamics. Early compartmental models focused on the natural history of infection, dividing populations into susceptible, infected, and clinical states, and incorporating age structure to predict prevalence trends and evaluate interventions such as treatment [6]. These models provide a foundation for incorporating drug-resistant strains, allowing researchers to simulate how resistance impacts transmission and disease burden [25].

Liu et al. [7] developed a within-host model and explored interactions between sensitive and resistant strains under antibiotic therapy. They integrated immune response dynamics and treatment outcomes to understand persistence and eradication failure using antibiotics.

At the population level, models incorporating resistance allow for the exploration of treatment effects, resistance emergence, and strain competition. Malfertheiner et al. [12] did research on the management of *H. pylori* infection and demonstrated that an age-structured compartmental model that includes both sensitive and resistant *H. pylori* infections can project infection prevalence and resistance trends under different intervention strategies. Insights from antimicrobial resistance modeling in other pathogens provide methodological guidance, emphasizing the inclusion of resistant compartments, fitness costs, and treatment failure rates [6, 25]. Computational and genomic studies done by [4] predict resistant phenotypes from sequence data, providing critical parameters for modeling transmission and intervention outcomes.

Previous modeling studies have also explored alternative approaches. Cousins et al. [10] formulated a model on the dynamics of Campylobacter, considering direct and indirect pathways, which assumed the insect vector as a mechanical vector for disease transmission. Rupnow et al. [15] developed an SEIR compartmental model to study the dynamics of *H. pylori* infection in the United States. Their findings highlighted projected infection trends, although the study did not consider environmental-to-human pathogen transmission.

Kirschner & Blaser [16] developed a deterministic model of *H. pylori* infection in the human stomach, focusing on mechanisms of bacterial persistence via an inflammation-driven autoregulatory network. In their model, the population consisted of gastric epithelial cells and bacteria, and the results demonstrated steady-state solutions robust to biological variation.

Malfertheiner et al. [11] reported that *H. pylori* infection results from complex bacterial virulence, host immune responses, and environmental factors. They noted that treatment combines strong acid suppressants with antibiotics and/or bismuth, and emphasized that rising antibiotic resistance necessitates susceptibility testing, resistance monitoring, and antibiotic stewardship.

Mutua et al. [9] developed a mathematical model to simulate *H. pylori* treatment and transmission and examined its implications for stomach cancer dynamics. Their findings indicated that increasing the treatment rate of *H. pylori* infections plays a vital role in reducing both the prevalence of the infection and the incidence of stomach cancer within the community. However, the study did not distinguish infectious individuals into drug-sensitive and drug-resistant categories, nor did it account for the occurrence of stomach ulcers. In this study, we extend their framework by introducing compartments for drug-sensitive infections, drug-resistant infections, and stomach ulcer cases, allowing a more comprehensive analysis of transmission dynamics, resistance development,

and intervention effectiveness. We model two antibiotic regimens for the treatment of *H. pylori* infection: (1) *first-line* antibiotics for individuals infected with the drug-sensitive strain, and (2) *second-line* antibiotics for individuals infected with the drug-resistant strain. In addition, individuals who develop stomach ulcers require a guided, combination-based treatment approach. By capturing the coexistence of sensitive and resistant strains, the model explores how antibiotic strategies influence resistance emergence and overall infection dynamics, providing insight into controlling multidrug-resistant *H. pylori* and reducing the burden of ulcers while addressing the growing challenge of antimicrobial resistance.

2. Model Formulation

Our *H. pylori* model considers the human population and the bacterial population. The human population $N(t)$ was divided into five epidemiological compartments at time, t: Susceptible individuals, S(t); Individuals infected with a drug-sensitive strain of *H. pylori,* $I_S(t)$; Individuals infected with a drug-resistant strain of *H. pylori,* $I_R(t)$; Individuals infected with stomach ulcers, $U(t)$ and recovered individuals, $R(t)$. Thus,

$$N(t) = S(t) + I_S(t) + I_R(t) + U(t) + R(t)$$

The bacterial concentration of *H. pylori* $D_H(t)$, in the environment are incorporated into the model as well. The formulation of this work is an extension of work carried out by Mutual et al. [9]. *H. pylori* is acquired through direct transmission or indirect transmission. Human-to-human transmission is direct transmission, whilst environment-to-human is indirect transmission. An infected individual can transmit *H. pylori* bacteria through contact with a susceptible individual, resulting in human-to-human. A susceptible individual can acquire *H. pylori* through ingesting the bacterial *H. pylori*, possibly through contaminated food, or water or drink to achieve environmental –to-human transmission. The force of infection along the direct transmission route is given by;

$$\lambda_{H_1} = \beta(I + \eta_1 I_R + \eta_2 U)$$

Whereas the force of infection along the indirect transmission through is given by:

$$\lambda_{H_2} = (1-\varepsilon)\frac{\nu_H D_H}{\kappa + D_H}$$

The parameter β denotes the human-to-human transmission rate between susceptible individuals and *H. pylori-infected* individuals. The modification parameters, η_1 *and* η_2, account for the relative infectiousness of individuals among individuals in I_R and U classes, respectively. We assume that $\eta_1, \eta_2 < 1$ to reflect the reduced infectiousness of individuals with drug-resistant H. pylori infections and those with stomach ulcers compared to individuals infected with the drug-sensitive strain.

The parameter ν_H represents the ingestion rate of *H. pylori* from *H. pylori-contaminated* environments with susceptible individuals. Parameter κ denotes the concentration of *H. pylori* in food or water along the indirect route, and ε represents the level of hygiene, safe water, and sanitation. The term $\frac{D_H}{\kappa + D_H}$ represents the probability of human consuming contaminated foods or water containing *H. pylori* bacteria.

When susceptible are exposed to *H. pylori,* causing bacteria, they either acquire a drug-sensitive strain with probability α or the drug-resistant strain with a $1-\alpha$ proportional with a progression rate of ω. Individuals,, $I_S(t)$ class recover following *first-line antibiotic* treatment at a rate of θ_S or develop drug-resistance and transition to the $I_R(t)$ class at a rate δ_S. Those in $I_R(t)$ class, may revert to $I_S(t)$ after *second- line antibiotic treatment* at a rate of δ_R, while treatment failure leads to stomach ulcer complications $U(t)$ at rate Ω. The shift from drug-resistant to drug-sensitive cases reflects a population-level effect in which treatment suppresses resistant strains, allowing sensitive strains to dominate or be detected clinically [28].

Stomach ulcer patients recover at a rate θ_U and move to the recovered class $R(t)$. Natural death, μ occurs in all human compartments, with additional disease-induced mortality rates $\kappa_S, \kappa_R,$ and κ_U for the $I(t)$, $I_R(t)$ and $U(t)$ sub-classes, respectively.

Environmental bacterial concentration increases through shedding from infected individuals at rates ϕ_S, ϕ_R and ϕ_U from $I_S(t)$, $I_R(t)$, and $U(t)$ sub-classes, respectively, while bacteria die naturally at rate μ_H. The parameter Λ represents the recruitment into susceptible, while parameter μ represents the natural death rate. It is assumed that individuals mix homogeneously band that they are indistinguishable in each of the classes.

2.1. Assumption of the Models

The formulation of the new model will be guided by the following assumptions.

1) All susceptible individuals have an equal probability of infection through direct (human-to-human) or indirect (environment-to-human) transmission.
2) The birth rate and natural death rate are not equal, and recruitment into the susceptible class occurs through birth or immigration.
3) Drug-resistant individuals recover only if they respond to *second-line* antibiotic treatment, first transitioning to the drug-sensitive class before moving to the recovered class.
4) Drug-resistant individuals who do not respond to *second-line* antibiotic treatment may die from the disease or develop stomach ulcers.

5) Recovered individuals do not acquire permanent immunity and can become susceptible again.
6) Infectious individuals shed bacteria into the environment, increasing environmental bacterial concentration.

Based on the variables, parameters, and assumptions, the schematic diagram illustrating the transmission dynamics of *H. pylori* with drug resistance is presented in Figure 1.

2.2. Schematic Diagram

The model formulation is summarized from by the schematic diagram 1 and six state dynamical system, developed from the diagram.

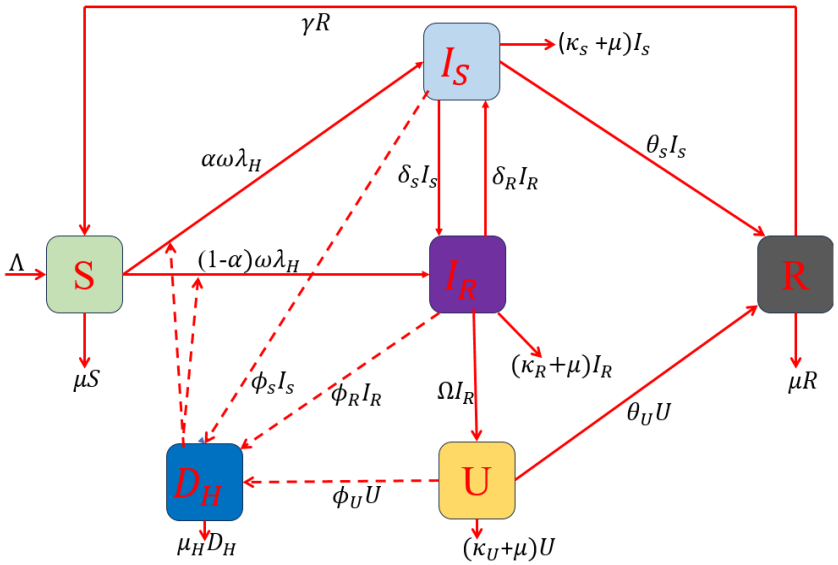

Figure 1. *A schematic diagram of the dynamic transmission of H. pylori with drug resistance.*

2.3. Model Equations

From the schematic diagram presented in Figure 1, we associate the following dynamical systems.

$$\frac{dS}{dt} = \Lambda + \gamma R(t) - (\lambda_H + \mu)S(t)$$

$$\frac{dI_S}{dt} = \alpha\omega\lambda_H S(t) + \delta_R I_R(t) - (\delta_S + \theta_S + \kappa_S + \mu)I_S(t)$$

$$\frac{dI_R}{dt} = (1-\alpha)\omega\lambda_H S(t) + \delta_I I(t) - (\delta_R + \Omega + \kappa_R + \mu)I_R(t)$$

$$\frac{dU}{dt} = \Omega I_R(t) - (\theta_U + \kappa_U + \mu)U(t) \quad (1)$$

$$\frac{dR}{dt} = \theta_S I(t) + \theta_U U(t) - (\gamma + \mu)R(t)$$

$$\frac{dD_H}{dt} = (1-\varepsilon)(\phi_S I_S + \phi_R I_R + \phi_U U)(t) - \mu_H D_H(t)$$

With initial conditions:

$$S(0) = S_O > 0, I_S(0) = I_{SO} > 0, I_R(0) = I_{R_O} > 0, U(0) = U_0 > 0, R(0) = R_O > 0, D_H(0) = D_{H_O} > 0. \quad (2)$$

To ensure readability, we make use of this notation: $\lambda_H = \lambda_{H_1} + \lambda_{H_2}$

3. Model Analysis

In this section, we show that the model is well posed. To achieve this, we prove positivity and boundedness of solutions of the model (1), determine the invariant region, equilibrium points, reproduction numbers, and stability analysis.

3.1. Invariant Region

We obtain the invariant region, in which model solutions are bounded. To do this, first divided the model system into two parts; Human population R_N and the concentration of bacteria from the environment R_{D_H} such that:

$$R_N = \{S(t), I_S(t), I_R(t), U(t), R(t)\} \in R_+^5 \text{ and } R_{D_H} = \{D_H(t)\} \in R_+^1$$

Total human population (N) at time t, given as:

$$N(t) = S(t) + I_S(t) + I_R(t) + U(t) + R(t) \quad (3)$$

Differentiating equation (3) w.r.t time yields:

$$\frac{dN}{dt} = \frac{dS}{dt} + \frac{dI_S}{dt} + \frac{dI_R}{dt} + \frac{dU}{dt} + \frac{dR}{dt} \quad (4)$$

In the absence of mortality due to *H. pylori* infection equation (4) i.e $(\kappa_S = \kappa_R = \kappa_U = 0)$ reduces to:

$$\frac{dN}{dt} \leq \Lambda - \mu N(t) \quad (5)$$

Integrating both sides of equation (5) yields:

$$\int \frac{dN}{\Lambda - \mu N(t)} \leq \int_0^t dt \quad (6)$$

Using the method of separation of variables of inequality and integrating equation (6), gives:

$$\frac{1}{-\mu} ln\{\Lambda - N(t)\} \leq t + c \quad (7)$$

$$\Rightarrow \frac{1}{-\mu}\{\Lambda - \mu N(t)\} \leq e^t * e^C \quad (8)$$

Now let $e^{-\mu C} = A$ and making $N(t)$ the subject in equation (8) becomes:

$$N(t) \geq \frac{\Lambda}{\mu} - \frac{Ae^{-\mu t}}{\mu} \quad (9)$$

Where A is a constant. By applying the initial condition at $t = 0$ and $N(0) = N_O$ in equation (9) and re-arranging gives:

$$N(t) \leq \frac{\Lambda}{\mu} - \left[\frac{\Lambda - \mu N_O}{\mu}\right] e^{-\mu t} \quad (10)$$

As $t \to \infty$, in equation (10) the human population size becomes $N \to \frac{\Lambda}{\mu,}$ which implies that that $0 \leq N \leq \frac{\Lambda}{\mu}$.

Therefore, the human population is bounded in the domain. $R_N = \{S, I_S, I_R, U, R\} \in R_+^5 : 0 \leq N \leq \frac{\Lambda}{\mu}$

Consider the bacteria concentration population at time t. Using the last equation of the model (1) and rearranging gives:

$$\frac{dD_H}{dt} + \mu_H D_H(t) \leq M(t) \quad (11)$$

Where $M(t) = (1 - \varepsilon)(\phi_S I_S + \phi_R I_R + \phi_U U)(t)$ is the bacterial recruitment rate in the environment. Now integrating (11) and rearranging yields:

$$D_H(t) = \frac{M(t)}{\mu_H} - \int \frac{M'(t)}{\mu_H} dt + \frac{\int udv - C}{e^{\mu_H t}} \quad (12)$$

As $t \to \infty$, in equation (12), the bacterial population size in environment $D_H \to \frac{M}{\mu_H}$, which implies that: $0 \leq D_H \leq \frac{M}{\mu_H}$.

Hence $R_H = \{D_H \in R_+^1\} : 0 \leq D_H \leq \frac{M}{\mu_H}$. Therefore, the whole model is bounded as:

$$\mathbb{Q} = \left\{S, I_S, I_R, U, R, D_H \geq 0 : N \leq \frac{\Lambda}{\mu};\ D_H \leq \frac{M}{\mu_H}\right\}$$

Therefore, the basic model is well posed epidemiologically and mathematically. Hence, it is sufficient to study the dynamics of the basic model in $\mathbb{Q}$.

3.2. Positivity of the Solutions

The model system (1) describes the dynamics of the human and bacterial population. We assume that the initial condition of the model are non-negative and its solutions must remain positive for all $t > 0$, as demonstrated in Theorem 1.

Theorem 1: The feasible region defined as $\mathbb{Q} = \{S(t), I_S(t), I_R(t), U(t), R(t), D_H(t)\} \in R_+^6$ *with initial conditions* $S(0) \geq 0, I(0) \geq 0, \geq 0, I_R(0) \geq 0, U(0) \geq 0, R(0) \geq 0, D_H(0)$ *then the solutions of* $\{S, I_S, I_R, U, R, D_H\}$ *are positive for* $t \geq 0$.

Proof: From the system of differential equations (1), let us take the first equation:

$$\frac{dS}{dt} = \Lambda + \gamma R(t) - (\lambda_H + \mu)S(t) \quad (13)$$

By the comparison theorem, equation (13) can be rewritten as:

$$\frac{dS}{dt} \geq -(\lambda_H + \mu)S(t) \quad (14)$$

Separating variables and integrating from 0 to t yields:

$$\therefore S(t) \geq S(0)e^{-(\lambda_H + \mu)t} \geq 0 \quad (15)$$

Equation (15) proves that the solution of equation (13) remains positive, provided that $S(0) \geq 0$.

Similarly, it can be shown that the solutions for the other model equation in system (1) are also non-negative. Thus, the solution set;

$$\{S(t), I_S(t), I_R(t), U(t), R(t), D_H(t)\} \geq 0 \forall\ t > 0 \quad (16)$$

This completes the proof of the theorem. Therefore, the solution of the model is positive.

3.3. Disease-Free Equilibrium Point (DFE)

To determine the disease-free equilibrium point (DFE) we equated the right-hand side of model (1) to zero, evaluated at $I_S = I_R = U = R = D_H = 0$, and solving for the noninfectious state variable [5].

Therefore, the disease-free equilibrium $B^O = \left(\frac{\Lambda}{\mu}, 0,0,0,0\right)$.

3.4. Control Reproduction Number

The control reproduction number is defined as the expected number of secondary infections produced by a single infected individual over their entire infectious period in a population that is not entirely susceptible due to control measures [18]. The Next-Generation Matrix method, as described by [19], is used to compute the control reproduction number, which is determined as the spectral radius of the matrix. The model equations are rewritten starting with newly infective classes:

$$\frac{dI_S}{dt} = \alpha\omega\lambda_H S(t) + \delta_R I_R(t) - (\delta_S + \theta_S + \kappa_S + \mu)I_S(t)$$

$$\frac{dI_R}{dt} = (1-\alpha)\omega\lambda_H S(t) + \delta_S I_S(t) - (\delta_R + \Omega + \kappa_R + \mu)I_R(t)$$

$$\frac{dU}{dt} = \Omega I_R(t) - (\theta_U + \kappa_U + \mu)U(t) \tag{17}$$

$$\frac{dD_H}{dt} = (1-\varepsilon)(\phi_S I_S + \phi_R I_R + \phi_U U)(t) - \mu_H D_H(t)$$

Then, by the principle of the next-generation matrix, we obtained

$$f = \begin{bmatrix} \alpha\omega\lambda_H S \\ (1-\alpha)\omega\lambda_H S \\ 0 \\ 0 \end{bmatrix}, \tag{18}$$

$$v = \begin{bmatrix} -\delta_R I_R + (\delta_S + \theta_S + \kappa_S + \mu)I_S \\ -\delta_S I_S + (\delta_R + \Omega + \kappa_R + \mu)I_R \\ -\Omega I_R + (\theta_U + \kappa_U + \mu)U \\ (1-\varepsilon)(\phi_S I_S + \phi_R I_R + \phi_U U) - \mu_H D_H \end{bmatrix},$$

The Jacobian matrices of f and v evaluated at DFE are given by F and V, respectively, such that;

$$F = \begin{bmatrix} \alpha\omega\beta S^0 & \alpha\omega\beta\eta_1 S^0 & \alpha\omega\beta\eta_2 S^0 & \frac{\alpha\omega S^0(1-\varepsilon)\nu_H}{\kappa} \\ (1-\alpha)\omega\beta S^0 & (1-\alpha)\omega\beta\eta_1 S^0 & (1-\alpha)\alpha\omega\beta\eta_2 S^0 & \frac{(1-\alpha)\omega S^0(1-\varepsilon)\nu_H}{\kappa} \\ 0 & 0 & 0 & 0 \\ 0 & 0 & 0 & 0 \end{bmatrix}, \tag{19}$$

$$V = \begin{bmatrix} t_1 & -\delta_R & 0 & 0 \\ -\delta_S & t_2 & 0 & 0 \\ 0 & -\Omega & t_3 & 0 \\ -(1-\varepsilon)\phi_S & -(1-\varepsilon)\phi_R & -(1-\varepsilon)\phi_U & \mu_H \end{bmatrix},$$

Where $t_1 = \delta_S + \theta_S + \kappa_S + \mu, t_2 = \delta_R + \Omega + \kappa_R + \mu, t_3 = \theta_U + \kappa_U + \mu$
The inverse of V is evaluated and given by:

$$V^{-1} = \begin{bmatrix} \frac{t_2}{\Delta} & \frac{\delta_R}{\Delta} & 0 & 0 \\ \frac{\delta_S}{\Delta} & \frac{t_1}{\Delta} & 0 & 0 \\ \frac{\Omega\delta_S}{\Delta t_3} & \frac{\Omega t_I}{\Delta t_3} & \frac{1}{t_3} & 0 \\ \frac{(1-\varepsilon)}{\Delta\mu_H}\left(\phi_S t_2 + \phi_R\delta_S + \phi_U\frac{\Omega\delta_S}{t_3}\right) & \frac{(1-\varepsilon)}{\Delta\mu_H}\left(\phi_S\delta_R + \phi_R t_1 + \phi_U\frac{\Omega t_1}{t_3}\right) & \frac{(1-\varepsilon)\phi_U}{t_3\mu_H} & \frac{1}{\mu_H} \end{bmatrix} \tag{20}$$

Where $\Delta = t_2 t_1 - \delta_S\delta_R$
Then,

$$FV^{-1} = \begin{bmatrix} \alpha\omega S^0 y_1 & \alpha\omega S^0 y_2 & \alpha S^0 y_3 & \frac{\alpha\omega S^0(1-\varepsilon)\nu_H}{\mu_H\kappa} \\ (1-\alpha)\omega S^0 y_1 & (1-\alpha)\omega S^0 y_2 & (1-\alpha)\omega\alpha S^0 y_3 & \frac{(1-\alpha)\omega S^0(1-\varepsilon)\nu_H}{\mu_H\kappa} \\ 0 & 0 & 0 & 0 \\ 0 & 0 & 0 & 0 \end{bmatrix} \tag{21}$$

Where;

$$y_1 = \frac{\beta t_2}{\Delta} + \frac{\beta\eta_1\delta_S}{\Delta} + \frac{\beta\eta_2\Omega\delta_S}{\Delta t_3} + \frac{(1-\varepsilon)\nu_H}{\kappa}.\frac{(1-\varepsilon)}{\Delta\mu_H}\left(\phi_S t_2 + \phi_R\delta_S + \phi_U\frac{\Omega\delta_S}{t_3}\right)$$

$$y_2 = \frac{\beta\delta_R}{\Delta} + \frac{\beta\eta_1 t_1}{\Delta} + \frac{\beta\eta_2\Omega t_1}{\Delta t_3} + \frac{(1-\varepsilon)\nu_H}{\kappa}.\frac{(1-\varepsilon)}{\Delta\mu_H}\left(\phi_S\delta_R + \phi_R t_1 + \phi_U\frac{\Omega t_1}{t_3}\right)$$

$$y_3 = \frac{\beta\eta_2}{t_3} + \frac{(1-\varepsilon)\nu_H}{\kappa} \cdot \frac{(1-\varepsilon)\phi_U}{t_3\mu_H}$$

The characteristic equation of FV^{-1} is obtained as;

$$\lambda^4 - \lambda^3 S^0(\alpha\omega y_1 + (1-\alpha\omega)y_2) = 0 \quad (22)$$

The eigenvalues of FV^{-1} are:

$$\lambda_1 = \lambda_2 = \lambda_3 = 0, \quad (23)$$

$$\lambda_4 = S^0\omega(\alpha y_1 + (1-\alpha)y_2),$$

The dominant eigenvalue of FV^{-1} is λ_4.

The dominant eigenvalue, corresponding to the spectral radius $\rho(FV^{-1})$, gives the control reproduction number [17], $\Re_c$, after substituting back y_1, y_2, S^0, t_1, t_2, and Δ in equation (24) yields:

$$\Re_c = \frac{\Lambda\omega}{\mu[(\delta_S+\theta_S+\kappa_S+\mu)(\delta_R+\Omega+\kappa_R+\mu)-\delta_S\delta_R]}\left\{\alpha\left[\beta(\delta_R+\Omega+\kappa_R+\mu)+\beta\eta_1\delta_S+\frac{\beta\eta_2\Omega\delta_S}{(\theta_U+\kappa_U+\mu)}+\frac{(1-\varepsilon)^2\nu_H}{\kappa\mu_H}\left(\phi_S t_2+\phi_R\delta_S+\phi_U\frac{\Omega\delta_S}{(\theta_U+\kappa_U+\mu)}\right)\right]+(1-\alpha)\left[\beta\delta_R+\beta\eta_1(\delta_S+\theta_S+\kappa_S+\mu)+\frac{\beta\eta_2\Omega(\delta_S+\theta_S+\kappa_S+\mu,)}{(\theta_U+\kappa_U+\mu)}+\frac{(1-\varepsilon)^2\nu_H}{\kappa\mu_H}\left(\phi_S\delta_R+\phi_R(\delta_S+\theta_S+\kappa_S+\mu)+\phi_U\frac{\Omega(\delta_S+\theta_S+\kappa_S+\mu)}{(\theta_U+\kappa_U+\mu)}\right)\right]\right\} \quad (24)$$

Therefore, the control reproduction number $(\Re_c)$for the *H. Pylori* system is expressed as:

$$\Re_c^* = \Re_{oS} + \Re_{Ro} \quad (25)$$

Thus, $(\Re_{oS})$ is the contribution of the drug-sensitive strain, given as;

$$\Re_S = \frac{\alpha\omega\Lambda}{\mu[(\delta_S+\theta_S+\kappa_S+\mu)(\delta_R+\Omega+\kappa_R+\mu)-\delta_S\delta_R]}\left\{\beta\left[\delta_R+\Omega+\kappa_R+\mu+\eta_1\delta_S+\frac{\eta_2\Omega\delta_S}{(\theta_U+\kappa_U+\mu)}\right]+\frac{(1-\varepsilon)^2\nu_H}{\kappa\mu_H}\left(\phi_S t_2+\phi_R\delta_S+\phi_U\frac{\Omega\delta_S}{(\theta_U+\kappa_U+\mu)}\right)\right\} \quad (26)$$

Likewise, $(\Re_{Ro})$ is the contribution of the drug-resistant strain is given as:

$$\Re_R = \frac{(1-\alpha)\omega\Lambda}{\mu[(\delta_S+\theta_S+\kappa_S+\mu)(\delta_R+\Omega+\kappa_R+\mu)-\delta_S\delta_R]}\left\{\beta\left[\delta_R+\eta_1(\delta_S+\theta_S+\kappa_S+\mu)+\frac{\eta_2\Omega(\delta_S+\theta_S+\kappa_S+\mu,)}{(\theta_U+\kappa_U+\mu)}\right]+\frac{(1-\varepsilon)^2\nu_H}{\kappa\mu_H}\left(\phi_S\delta_R+\phi_R(\delta_S+\theta_S+\kappa_S+\mu)+\phi_U\frac{\Omega(\delta_S+\theta_S+\kappa_S+\mu)}{(\theta_U+\kappa_U+\mu)}\right)\right\} \quad (27)$$

3.5. Local Stability of Disease-Free Equilibrium

The local stability of the disease-free equilibrium is a critical aspect of analyzing the dynamics of infectious diseases within a population. This stability analysis helps determine whether small perturbations around the disease-free state cause the system to return to equilibrium or diverge towards disease prevalence [23]. The following theorem illustrates the stability of the disease-free equilibrium point:

Theorem 2. The disease-free equilibrium point is locally asymptotically stable if $\Re_0 < 1$ *and unstable if* $\Re_0 > 1$.

Proof. To prove local stability of the disease-free equilibrium, we obtained the Jacobian matrix of the system (1) at the disease-free equilibrium E_O:

$$J(E^O) = \begin{bmatrix} -\mu & -\frac{\Lambda\beta}{\mu} & -\frac{\Lambda\beta\eta_1}{\mu} & -\frac{\Lambda\beta\eta_2}{\mu} & \gamma & -\frac{\Lambda(1-\varepsilon)\nu_H}{\kappa\mu} \\ 0 & \frac{\Lambda\alpha\beta\omega}{\mu}-k_1 & \frac{\Lambda\alpha\beta\eta_1\omega}{\mu}+\delta_R & \frac{\Lambda\alpha\beta\eta_2\omega}{\mu} & 0 & \frac{\Lambda\alpha\omega(1-\varepsilon)\nu_H}{\kappa\mu} \\ 0 & -\frac{\Lambda\beta\omega(1-\alpha)}{\mu}+\delta_S & -\frac{\Lambda\beta\eta_1\omega(1-\alpha)}{\mu}-k_2 & \frac{\Lambda\beta\eta_2\omega(1-\alpha)}{\mu} & 0 & -\frac{\Lambda\omega(1-\alpha)(1-\varepsilon)\nu_H}{\kappa\mu} \\ 0 & 0 & \Omega & -k_3 & 0 & 0 \\ 0 & \theta_S & 0 & \phi_U & -k_4 & 0 \\ 0 & (1-\varepsilon)\phi_S & (1-\varepsilon)\phi_R & (1-\varepsilon)\phi_U & 0 & -\mu_H \end{bmatrix} \quad (28)$$

Where $k_1 = \delta_s + \theta_S + \kappa_s + \mu$, $k_2 = \delta_R + \Omega + \kappa_R + \mu$ $k_3 = \theta_U + \kappa_U + \mu$ and $k_4 = \gamma + \mu$

From the Jacobian matrix of (28), we obtained a characteristic polynomial.

$$\lambda^2 + (\mu + k_4)\lambda + \mu k_4 = 0 \quad (29)$$

By Routh –Hurwitz criteria equation (29) has strictly negative roots, some of which are: $\lambda = -\mu$ and $\lambda = -k_4$

The remaining part of the characteristic polynomial in equation (28) is:

$$\lambda^4 + a_1\lambda^3 + a_2\lambda^2 + a_3\lambda + a_4 = 0 \quad (30)$$

Where a_1, a_2, a_3 and a_4 are determined as follows:

$$a_1 = k_1 + k_2 + k_3 + \mu_H - \frac{\Lambda\alpha\beta\omega}{\mu} + \frac{\Lambda\beta\eta_1\omega(1-\alpha)}{\mu}$$

$$a_2 = k_1k_2 + k_1k_3 + k_2k_3 + \mu_H(k_1 + k_2 + k_3) + k_3\mu_H - \frac{\Lambda\alpha\beta\omega}{\mu}(k_2 + k_3 + \mu_H) + \frac{\Lambda\beta\eta_1\omega(1-\alpha)}{\mu}(k_1 + k_3 + \mu_H) - \delta_R\delta_S - \Omega(1-\varepsilon)\phi_R$$

$$a_3 = k_1k_2k_3 + \mu_H(k_1k_2 + k_1k_3 + k_2k_3) - \frac{\Lambda\alpha\beta\omega}{\mu}(k_2k_3 + k_3\mu_H) + \frac{\Lambda\beta\eta_1\omega(1-\alpha)}{\mu}(k_1k_3 + k_3\mu_H) - \delta_R\delta_S(k_3 + \mu_H) - \Omega(1-\varepsilon)(\phi_Rk_1 + \phi_U\Omega)$$

$$a_4 = k_3k_2k_1\kappa\mu_H - k_3\delta_S\delta_R\kappa\mu_H + \frac{\Lambda}{\mu}\omega\alpha\beta k_3k_2\kappa\mu_H + \frac{\Lambda}{\mu}\omega\alpha\beta\eta_1\delta_Sk_3\kappa\mu_H + \frac{\Lambda}{\mu}\omega\alpha\beta\eta_2\Omega\delta_S\kappa\mu_H + (1-\alpha)\frac{\Lambda}{\mu}\omega\beta\delta_Rk_3\kappa\mu_H + (1-\alpha)\frac{\Lambda}{\mu}\omega\beta\eta_1k_1k_3\kappa\mu_H + \frac{\Lambda}{\mu}\omega(1-\alpha)\beta\eta_2\Omega k_1\kappa\mu_H + \frac{\Lambda}{\mu}\omega\alpha(1-\varepsilon)^2\nu_Hk_3\left(\phi_Sk_2 + \phi_R\delta_S + \phi_U\frac{\Omega\delta_S}{t_3}\right) + \frac{\Lambda}{\mu}\omega(1-\alpha)(1-\varepsilon)^2\nu_Hk_3\left(\phi_S\delta_R + \phi_Rk_1 + \phi_U.\frac{\Omega k_1}{k_3}\right)$$

We applied the Routh–Hurwitz criteria. By the principle of Routh-Hurwitz criteria equation (30) has strictly negative real roots if and only if $a_1 > 0, a_2 > 0, a_3 > 0$ and $a_4 > 0$,

By the Routh-Hurwitz criteria,

$a_1 > 0$ Means that,

$$k_1 + k_2 + k_3 + \mu_H > -\frac{\Lambda\alpha\beta\omega}{\mu}(\alpha - (1-\alpha))$$

Also $a_2 > 0,$ mean that,

$$k_1k_2 + k_1k_3 + k_2k_3 + \mu_H(k_1 + k_2 + k_3) + k_3\mu_H > \frac{\Lambda\beta\omega}{\mu}[\alpha(k_2 + k_3 + \mu_H) - (1-\alpha)\eta_1(k_1 + k_3 + \mu_H)] + \delta_R\delta_S + \Omega(1-\varepsilon)\phi_R$$

Also $a_3 > 0,$ mean that,

$$k_1k_2k_3 + \mu_H(k_1k_2 + k_1k_3 + k_2k_3) > \frac{\Lambda\alpha\beta\omega}{\mu}[\alpha(k_2 + \mu_H) - (1-\alpha)\eta_1(k_1 + \mu_H)] + \Omega(1-\varepsilon)(\phi_Rk_1 + \phi_U\Omega)$$

Also $a_4 > 0,$ which means that,

On rearranging a_4 yields:

$$k_3\kappa\mu_H(k_2k_1 - \delta_S\delta_R) > \frac{\Lambda\omega}{\mu}\left\{\alpha\left(\beta k_3k_2\kappa\mu_H + \beta\eta_1\delta_Sk_3\kappa\mu_H + \beta\eta_2\Omega\delta_S\kappa\mu_H + (1-\varepsilon)^2\nu_Hk_3\left(\phi_Sk_2 + \phi_R\delta_S + \phi_U\frac{\Omega\delta_S}{k_3}\right)\right) + (1-\alpha)\left(\beta\delta_Rk_3\kappa\mu_H + \beta\eta_1k_1k_3\kappa\mu_H + \beta\eta_2\Omega k_1\kappa\mu_H + (1-\varepsilon)^2\nu_Hk_3\left(\phi_S\delta_R + \phi_Rk_1 + \phi_U.\frac{\Omega k_1}{k_3}\right)\right)\right\} \quad (31)$$

On rearranging, the expression of equation (31) yields:

$$\frac{\Lambda\omega}{\mu(k_2k_1 - \delta_S\delta_R)}\left\{\alpha\left(\beta k_2 + \beta\eta_1\delta_S + \frac{\beta\eta_2\Omega\delta_S}{k_3} + \frac{(1-\varepsilon)^2\nu_H}{\kappa\mu_H}\left(\phi_Sk_2 + \phi_R\delta_S + \phi_U\frac{\Omega\delta_S}{t_3}\right)\right) + (1-\alpha)\left(\beta\delta_R + \beta\eta_1k_1 + \frac{\beta\eta_2\Omega k_1}{k_3} + \frac{(1-\varepsilon)^2\nu_H}{\kappa\mu_H}\left(\phi_S\delta_R + \phi_Rk_1 + \phi_U.\frac{\Omega k_1}{k_3}\right)\right)\right\} < 1 \quad (32)$$

However, the left-hand side of equation (32) defines the control reproduction number:

$$\Rightarrow \Re_c < 1 \quad (33)$$

Thus, the disease-free equilibrium is locally asymptotically stable if and only if $\Re_c < 1$.

From equation (33), the disease-free equilibrium is locally asymptotically stable if $\Re_c < 1$. This implies that each infectious individual infects, on average, less than one susceptible individual during the infectious period, leading to the eventual elimination of the disease.

3.6. The Endemic Equilibrium

The steady state at which *H. pylori* infection persists within the community is referred to as the endemic equilibrium of system (1). At this equilibrium, the rate of change of the population in each class is zero. Hence, the model system (1) can be represented as:

$$0 = \Lambda + \gamma R^* - (\lambda_{H_1} + \lambda_{H_2} + \mu)S^*$$

$$0 = \alpha\omega(\lambda_{H_1} + \lambda_{H_2})S^* + \delta_R I_R^* - (\delta_S + \theta_S + \kappa_S + \mu)I_S^*$$

$$0 = (1-\alpha)\omega(\lambda_{H_1} + \lambda_{H_2})S^* + \delta_S I_S^* - (\delta_R + \Omega + \kappa_R + \mu)I_R^*$$

$$0 = \Omega I_R^* - (\theta_U + \kappa_U + \mu)U^* \quad (34)$$

$$0 = \theta_S I_S^* + \theta_U U^* - (\gamma + \mu)R^*$$

$$0 = (1-\varepsilon)(\phi_S I_S^* + \phi_R I_R^* + \phi_U U^*) - \mu_H D_H^*$$

Now the steady state expressed S^*, I_S^*, I_R^*, U^*, R^* and D_H^* from equation (34) to get:

The endemic steady-state solution for system is given by:

$$B^* = (S^*, I_S^*, I_R^*, U^*, R^*, D_H^*) \quad (35)$$

where

$$S^* = \frac{\Lambda + \frac{\gamma}{\gamma+\mu}(\theta_S I_S^* + \theta_U U^*)}{\lambda_{H_1} + \lambda_{H_2} + \mu},\ I_S^* = \frac{\alpha\omega(\lambda_{H_1} + \lambda_{H_2})S^* + \delta_R I_R^*}{k_1},\ I_R^* = \frac{(1-\alpha)\omega(\lambda_{H_1} + \lambda_{H_2})S^* + \delta_S I_S^*}{k_3},$$

$$U^* = \frac{\Omega I_R^*}{k_4},\ R^* = \frac{\theta_S I_S^* + \theta_U U^*}{k_5},\ D_H^* = \frac{(1-\varepsilon)(\phi_S I_S^* + \phi_R I_R^* + \phi_U U^*)}{\mu_H}$$

Where $k_1 = \mu + \omega$, $k_2 = \delta_s + \theta_s + k_s + \mu$, $k_3 = \delta_R + \Omega + k_R + \mu, k_4 = \theta_U + k_U + \mu$ and $k_5 = \gamma + \mu$

3.7. Global Stability of the Endemic Equilibrium

In epidemiological modeling, the global stability of an endemic equilibrium implies that the disease will persist at a constant level over time, regardless of the initial state of the population, provided the initial conditions lie within a realistic and meaningful range [26]. This concept is crucial for understanding the long-term dynamics of disease transmission and for designing effective public health strategies. To prove the global asymptotic stability of the endemic equilibrium, the method of Lyapunov functions is employed. A logarithmic Lyapunov function used for this purpose is defined as follows:

$$L(S, I_S, I_R, U, R, D_H) = \left(S - S^* + S^* ln\frac{S^*}{S}\right) + \left(I_S - I_S^* + I_S^* ln\frac{I_S^*}{I_S}\right) + \left(I_R - I_R^* + I_R^* ln\frac{I_R^*}{I_R}\right) + \left(U - U^* + U^* ln\frac{U^*}{U}\right) + \left(R - R^* + R^* ln\frac{R^*}{R}\right) + \left(D_H - D_H^* + D_H^* ln\frac{D_H^*}{D_H}\right) \quad (36)$$

The derivative of L along the solution trajectories of system (1) is given by:

$$\frac{dL}{dt} = \left(\frac{S-S^*}{S}\right)\frac{dS}{dt} + \left(\frac{I_S - I_S^*}{I_S}\right)\frac{dI_S}{dt} + \left(\frac{I_R - I_R^*}{I_R}\right)\frac{dI_R}{dt} + \left(\frac{U-U^*}{U}\right)\frac{dU}{dt} + \left(\frac{R-R^*}{R}\right)\frac{dR}{dt} + \left(\frac{D_H - D_H^*}{D_H}\right)\frac{dD_H}{dt} \quad (37)$$

Substituting the expressions for $\frac{dS}{dt}, \frac{dI_S}{dt}, \frac{dI_R}{dt}, \frac{dU}{dt}, \frac{dR}{dt}, \frac{dD_H}{dt}$ from model system (1) into equation (38) and simplifying yields:

$$\frac{dL}{dt} = Q - K \quad (38)$$

Where

$$Q = \Lambda + \gamma R + \frac{\gamma R^* S^*}{S} + \alpha\omega(\lambda_{H_1} + \lambda_{H_2})S + \frac{\alpha\omega(\lambda_{H_1} + \lambda_{H_2})S^* I_S^*}{I_S} + \delta_R I_R + \frac{\delta_R I_R^* I_S^*}{I_S} + (1-\alpha)\omega(\lambda_{H_1} + \lambda_{H_2})S + \frac{(1-\alpha)\omega(\lambda_{H_1} + \lambda_{H_2})S^* I_R^*}{I_R}$$

$$+\delta_S I_S + \frac{\delta_S I_S^* I_R^*}{I_R} + \Omega I_R + \frac{\Omega I_R^* U^*}{U} + \theta_S I_S + \theta_U U + \frac{\theta_S I_S^* R^*}{R} + \frac{\theta_U U^* R^*}{R} + (1-\varepsilon)(\phi_S I_S + \phi_R I_R + \phi_U U) + \frac{(1-\varepsilon)(\phi_S I_S^* + \phi_R I_R^* + \phi_U U^*)D_H^*}{D_H}$$

$$K = \frac{\Lambda S^*}{S} + \gamma R^* + \alpha\omega(\lambda_{H_1} + \lambda_{H_2})S^* + \frac{\alpha\omega(\lambda_{H_1} + \lambda_{H_2})SI_S^*}{I_S} + \delta_R I_R^* + \frac{\delta_R I_R I_S^*}{I_S} + \theta_U U^* + \frac{\theta_S I_S R^*}{R} + \theta_S I_S^* + (1-\alpha)\omega(\lambda_{H_1} + \lambda_{H_2})S^* +$$
$$\frac{(1-\alpha)\omega(\lambda_{H_1} + \lambda_{H_2})SI_R^*}{I_R} + \delta_S I_S^* + \frac{\delta_S I_S I_R^*}{I_R} + \Omega I_R^* + \frac{\Omega I_R U^*}{U} + \frac{\theta_U U R^*}{R} + (1-\varepsilon)(\phi_S I_S^* + \phi_R I_R^* + \phi_U U^*) + \frac{(1-\varepsilon)(\phi_S I_S + \phi_R I_R + \phi_U U)D_H^*}{D_H} +$$
$$\frac{(S-S^*)^2}{S}(\lambda_{H_1} + \lambda_{H_2} + \mu) + \frac{(I_S - I_S^*)^2}{I_S}(\delta_S + \theta_S + \kappa_S + \mu) + \frac{(I_R - I_R^*)^2}{I_R}(\delta_R + \Omega + \kappa_R + \mu) + \frac{(U-U^*)^2}{U}(\theta_U + \kappa_U + \mu) +$$
$$\frac{(R-R^*)^2}{R}(\gamma + \mu) + \frac{\mu_H(D_H - D_H^*)^2}{D_H}$$

Thus if $Q < K$, then $\frac{dL}{dt} = 0$ if and only if $S = S^*, I_S = I_S^*, I_R = I_R^*, U = U^*, R = R^*, D_H = D_H^*$ Therefore, the largest compact invariant set in $\left\{(S^*, I_S^*, I_R^*, U^*, R^*, D^*) \in \Omega: \frac{dL}{dt} = 0\right\}$ is the singleton B^*, where B^* is the endemic equilibrium of the system (1).

By LaSalle's invariant principle [21], it follows that as $t \to \infty$, the solution of the model system (1) approaches the endemic equilibrium B^* when the control reproduction number $\Re_c^* > 1$.

Therefore, the endemic equilibrium point B^* is globally asymptotically stable in the invariant set Ω if $Q < K$.

3.8. Global Stability of Disease-Free Equilibrium

To investigate the global stability of disease free equilibrium in the model (1). The model is shown that it is globally-asymptotically stable of the (DFE). It is analyzed using the Castillo–Chavez method [20]. First the model (1) is re-written as:

$$\frac{dX}{dt} = F(X, Z)$$

$$\frac{dZ}{dt} = G(X, Z),\ G(X, 0) = 0 \tag{39}$$

Where $X = (S, R)$ and $Z = (I_s, I_R, U, D_H)^T$, with the components of $X \in R^{2+}$ representing the uninfected population and the components of $Z \in R^{4+}$ representing the infected population. Theorem 3. The disease- free equilibrium of the system (1) is globally asymptotically stable in $\mathbb{Q}$ if and only if $\Re_c < 1$ and the condition (T_1) and (T_2) are satisfied:

(T_1). For $\frac{dX}{dt} = F(X, 0), X^*$ is globally asymptotically stable.

(T_2). $G(X, Z) = AZ - \hat{G}(X, Z), \hat{G}(X, Z) \geq 0$ for $(X, Z) \in \mathbb{Q}$.

To verify condition (T_1) consider, the first and fifth equation of system (1) expressed as:

$$\frac{dS}{dt} = \Lambda + \gamma R(t) - (\lambda_H + \mu)S(t)$$

$$\frac{dR}{dt} = \theta_S I(t) + \theta_U U(t) - (\gamma + \mu)R(t) \tag{40}$$

If there is no infection in the population, equation (40) reduces to:

$$\frac{dX}{dt} = F(X, 0) = \Lambda - \mu S(t) \tag{41}$$

By use method of separation of variables and integrate equation (42) gives;

$$S^*(t) = \frac{\Lambda}{\mu} + \left(S^*(0) - \frac{\Lambda}{\mu}\right)e^{-\mu t} \tag{42}$$

It follows that, as $t \to \infty, S(t) \to N$ which establishes global asymptotic stability of the equilibrium $S^* = \frac{\Lambda}{\mu}$ corresponding to the disease-free equilibrium point $S^* = \left(\frac{\Lambda}{\mu}, 0,0,0,0,0\right)$.

Thus, X^* is globally asymptotically stable, hence condition one is satisfied.

Next, to verify second condition (T_2) by linearizing of the infected subsystem.

$$G(X, Z) = AZ - \hat{G}(X, Z), \hat{G}(X, Z) \geq 0 \text{ for } (X, Z) \in \Omega$$

Where $A = D_Z G(X, Z)$ which is a Metzler. Thus,

$$A = \begin{bmatrix} -(\delta_S + \theta_S + \kappa_S + \mu) & \delta_R & 0 & 0 & 0 \\ \delta_S & -(\delta_R + \Omega + \kappa_R + \mu) & 0 & 0 & 0 \\ 0 & \Omega & -(\theta_U + \kappa_U + \mu) & 0 & 0 \\ \theta_S & 0 & \theta_U & -(\gamma + \mu) & 0 \\ (1-\varepsilon)\phi_S & (1-\varepsilon)\phi_R & (1-\varepsilon)\phi_U & 0 & -\mu_H \end{bmatrix} \tag{43}$$

$$AZ = \begin{bmatrix} -(\delta_S + \theta_S + \kappa_S + \mu)I_S + \delta_R I_R \\ \delta_S I_S - (\delta_R + \Omega + \kappa_R + \mu)I_R \\ \Omega I_R - (\theta_U + \kappa_U + \mu)U \\ \theta_S I_S + \theta_U U - (\gamma + \mu)R \\ (1-\varepsilon)(\phi_S I_S + \phi_R I_R + \phi_U U) - \mu_H D_H \end{bmatrix} \tag{44}$$

$$G(X, Z) = \begin{bmatrix} -(\delta_S + \theta_S + \kappa_S + \mu)I_S + \delta_R I_R - \alpha\omega\lambda_H S \\ \delta_S I_S - (\delta_R + \Omega + \kappa_R + \mu)I_R - (1-\alpha)\omega\lambda_H S \\ \Omega I_R - (\theta_U + \kappa_U + \mu)U \\ \theta_S I_S + \theta_U U - (\gamma + \mu)R \\ (1-\varepsilon)(\phi_S I_S + \phi_R I_R + \phi_U U) - \mu_H D_H \end{bmatrix} \tag{45}$$

So that

$$\hat{G}(X,Z)=\begin{bmatrix}\hat{G}_1(X,Y)\\ \hat{G}_2(X,Y)\\ \hat{G}_3(X,Y)\\ \hat{G}_4(X,Y)\\ \hat{G}_5(X,Y)\end{bmatrix}=\begin{bmatrix}\alpha\omega\left[\beta(I_S+\eta_1 I_R+\eta_2 U)+(1-\varepsilon)\frac{\nu_H D_H}{\kappa+D_H}\right](S^o-S)\\ (1-\alpha)\omega\left[\beta(I_S+\eta_1 I_R+\eta_2 U)+(1-\varepsilon)\frac{\nu_H D_H}{\kappa+D_H}\right](S^o-S)\\ 0\\ 0\\ 0\end{bmatrix} \quad (46)$$

Thus, if $\hat{G}(X,Z)\geq 0$, then DFE is asymptotically stable and unstable otherwise. The susceptible is bounded as $S\leq S^o$. Therefore $\hat{G}_1(X,Y)\geq 0$, $\hat{G}_2(X,Y)\geq 0$, $\hat{G}_3(X,Y)=0$, $\hat{G}_4(X,Y)=0$ and $\hat{G}_5(X,Y)=0$. Thus, DFE is globally asymptotically stable when $\Re_o^*<1$. This demonstrates that, irrespective of the initial population of infected individuals, *H. pylori* infection can still be controlled.

3.9. Sensitivity Analysis of the Control Reproduction Number

In this section, a sensitivity analysis of the control reproduction number is presented to assess the relative importance of various parameters influencing the transmission and prevalence of *H. pylori* infection within the population. The normalized forward sensitivity index, as described in [23], is employed for this analysis. This index measures the relative change in the control reproduction number $\Re_C$ with respect to a given parameter m and is defined as:

$$\Upsilon_m^{\Re_C}=\frac{\partial\Re_C}{\partial m}\times\frac{m}{\Re_C} \quad (48)$$

The parameter values in Table 1 are used to calculate the sensitivity indices of $\Re_c$ with respect to the parameters $\Lambda,\beta,\alpha,\omega,\eta_1,\eta_2,\varepsilon,\delta_S,\delta_R,\Omega,\mu,\mu_H,\theta_S,\theta_U,\gamma,\kappa_S,\kappa_R$ and κ_U.

Table 1. *Baseline parameter values used in the H. pylori model.*

Parameter Symbol	Value	Source
Λ	10 month^{-1}	[9]
β	0.825 month^{-1}	[9]
ε	0.5	[9]
λ_{H_1}	0.2 month^{-1}	[9]
λ_{H_2}	0.1075 month^{-1}	[9]
α	0.65	Assumed
ω	0.0075	[23]
η_1	0.0286	[9]
η_2	0.0125	[9]
Ω	0.0025 month^{-1}	[12]
θ_S	0.615 month^{-1}	[6]
θ_U	0.175 month^{-1}	Assumed
δ_S	0.0839 month^{-1}	[22]
δ_R	0.0978 month^{-1}	[22]
κ_S	0.00264 month^{-1}	Assumed
κ_R	0.00134 month^{-1}	[6]
κ_U	0.0012 month^{-1}	Assumed
μ	0.000019 month^{-1}	[9]
μ_H	0.001 month^{-1}	[9]
γ	0.002485 month^{-1}	[9]
Φ_S	0.0008 month^{-1}	Assumed
Φ_R	0.0004 month^{-1}	Assumed
Φ_U	0.0839 month^{-1}	[9]

The computed sensitivity indices are presented in Table 2. A positive sensitivity index indicates that the reproduction number increases with an increase in the corresponding parameter, while a negative sensitivity index indicates that the reproduction number decreases as the parameter increases [9].

From Table 2, it is observed that the parameters $\Lambda,\beta,\eta_1,\eta_2$ *and* Ω have positive sensitivity index values, indicating that an increase in these parameters leads to a corresponding increase in the number of infected individuals. On the other hand $\delta_R,\delta_S,\mu,\mu_H,\kappa_S,\kappa_R,\kappa_U,\theta_U$, θ_S and γ have negative sensitivity index values, meaning that increasing these parameters results in a decrease in the number of infected individuals. For instance, if the transmission rate β increases by 10%, the reproduction number also increases by 10%. Conversely, increasing the rate developing antibiotic resistance δ_S for drug resistant individuals by 10% reduces $\Re_C$ by approximately 0.44314%, while increasing the antibiotic treatment efficacy θ_S by 10% decreases $\Re_C$ by approximately 0.25438%.

Table 2. *Sensitivity indices of the control reproduction number relative to selected model parameters.*

Parameter	Sensitivity index
Λ	+1
β	+1

Parameter	Sensitivity index
η_1	+0.40281
η_2	+0.129267
ε	+0.250130
Ω	+0.066953
δ_S	+0.031342
δ_R	+0.0420135
δ_S	−0.044314
θ_S	−0.025438
θ_U	−0.332071
γ	−0.074734

Parameter	Sensitivity index
κ_S	−0.074734
κ_R	−0.092307
κ_U	−0.0823450

4. Model Simulations

Numerical simulations of the system of model equation (1) were conducted to predict the epidemic behavior of *H. pylori* infection. These simulations were performed utilizing MATLAB's built-in ordinary differential equation solver, ode45. The parameter values used are provided in Table 1, and the initial state values are as follows:

$$\mathrm{S}(0) = 10000,\ I_S(0) = 7000, \mathrm{I_R}(0) = 3000, U(0) = 1500,\ \mathrm{R}(0) = 6000, D_H(0) = 5000.$$

These values were obtained from literature review [9, 12, 22, 23] and published Kenyan data [2, 3, 5, 27]. The simulations are conducted over a time span of 0 to 20 months, taking into account that *H. pylori* infections with drug-resistant strains often take a long time to reactivate into a drug-resistant strain disease and eventually be cured. The simulation results are presented graphically in Figures 2–4.

We display a graphical trend of the model with some parameter values remaining unchanged, while others are varied.

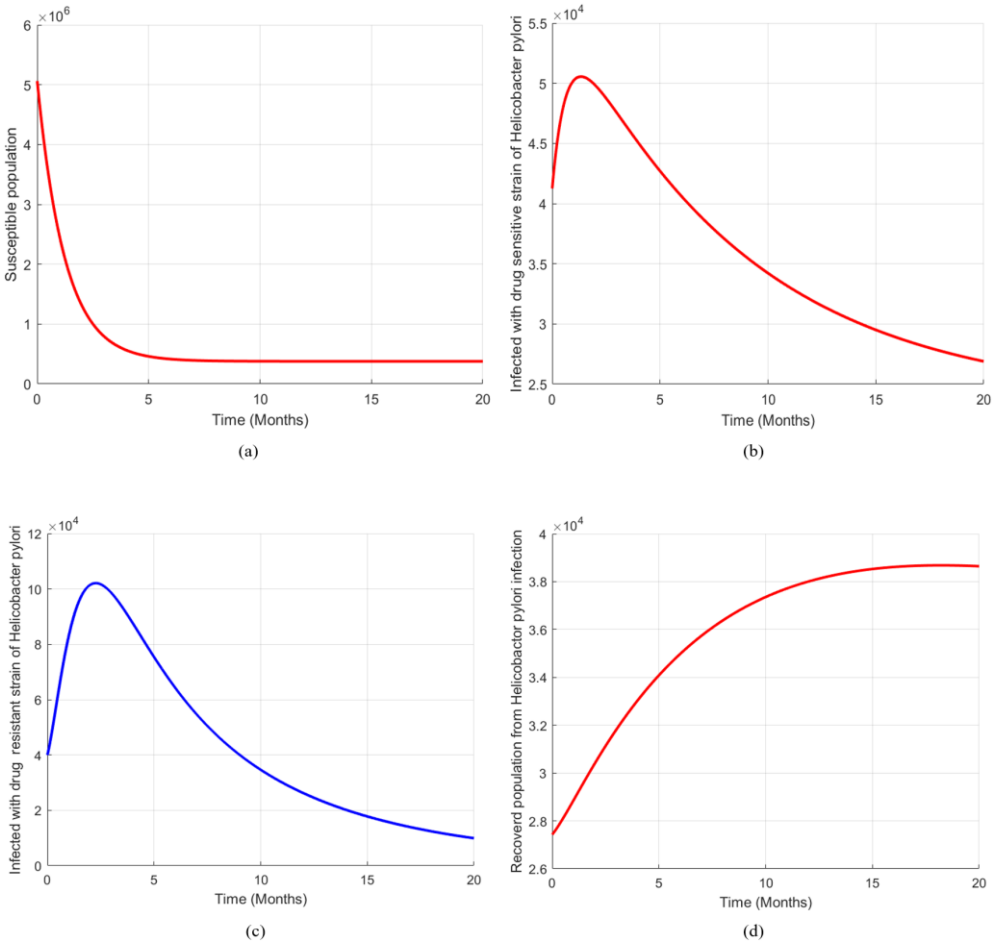

Figure 2. *Shows the simulation population on trajectories of susceptible, infected with drug-sensitive, infected with drug-resistant, and recovered individuals over time, presented in (a), (b), (c), and (d), respectively.*

Figure 2(a) examines the simulation of the susceptible population to *H. pylori* infection with time in months. The result indicates that initially susceptible individuals is very high, but it decreases rapidly as people get infected. Steep decline of the curve indicates strong transmission in the early phase of the epidemic, and after a few months, the curve levels off and approaches a constant value. The plateau represents a steady state (equilibrium) where new susceptible individuals (e.g., through recruitment or recovery) are balanced by infections and natural death. At this stage, the infection persists in the population at an endemic level, and the susceptible population no longer changes significantly with time.

Figure 2(b) illustrates the dynamics of individuals infected with the drug-sensitive strain of *H. pylori* over time. At first, the number of infected individuals increases, showing rapid transmission and an increase of the infection in the community. Transmission rate mainly depends on contact rate with infective individuals and also when ones does not observe hygiene and sanitation, especially when one is handling food, water, and drinks. After reaching a peak, the curve declines gradually, indicating that treatment, recovery, and natural removal reduce the infection rate in the population.

Figure 2(c) depicts the dynamics of drug-resistant *H. pylori* infections with time, which at the start increase and when reaches the peak, it starts gradually declining. The increase shows the emergence and spread of a resistance strain, while the consequent reduction indicates the combined effects of effective treatment, recovery, and minimized transmission of the bacteria. Administering appropriate antibiotics to infected individuals leads to a decline in the curve, which in turn improves recovery rates and the use of good hygiene practices, such as safe handling of food and drinking water.

Figure 2(d) illustrates a simulation of the recovered population from *H. pylori* with time in months. A steady increase in the recovered population over time reflects improved health outcomes. This is achieved through the use of appropriate antibiotics, which enhances treatment effectiveness, alongside good hygiene and sanitation practices, which greatly minimize further infection transmission in the population. Moreover, reduced contact rate with infected individuals lowers new infections, allowing more individuals to recover progressively until the system reaches a stable state.

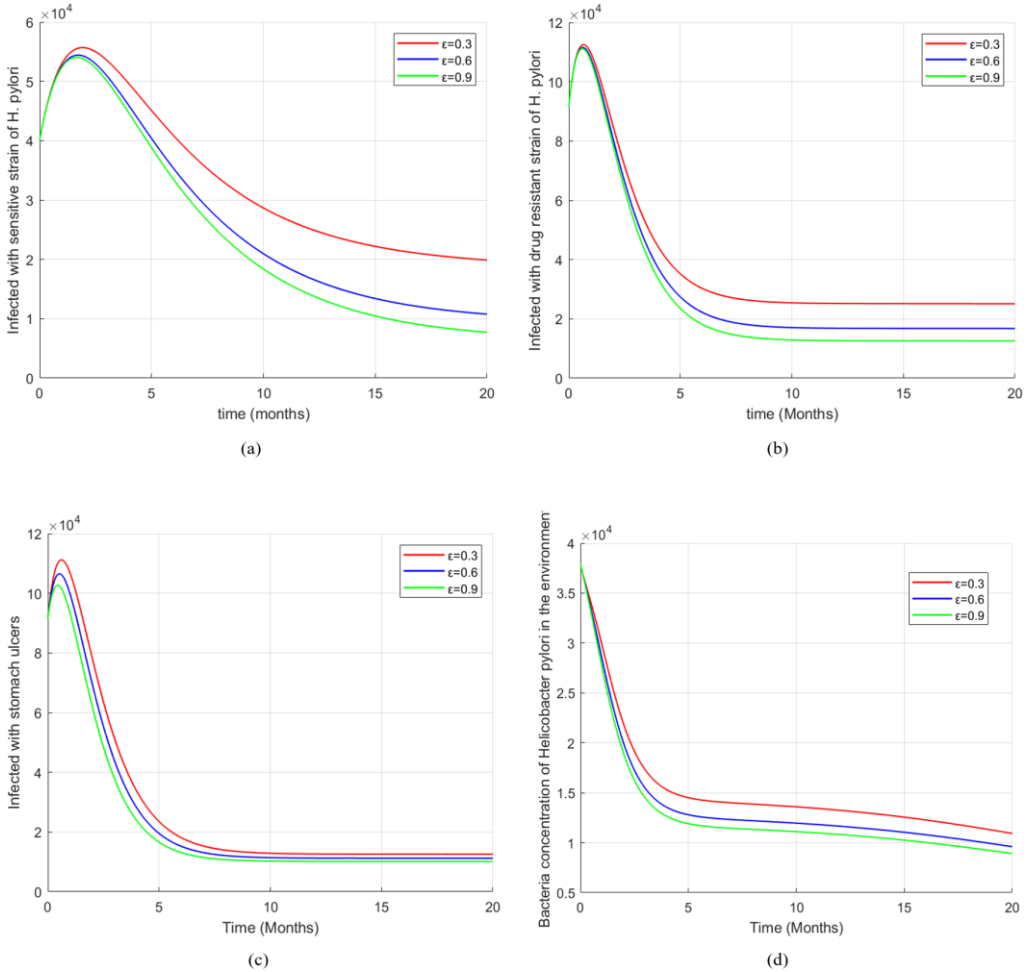

Figure 3. *Shows the effects of varying the parameter* (ε) *on the population trajectories of individuals with drug-sensitive infection, drug-resistant infection, stomach ulcers, and the environmental bacterial population, using the parameter values in Table 1. Results are presented in (a), (b), (c), and (d), respectively.*

Figure 3(a) illustrates the effect of varying hygiene and sanitation levels (ε) on an individual's sensitive *H. pylori* with time. The results show that those infected with the drug-sensitive *H. pylori* strain initially rise, and when it reaches the peak starts declining over time. It is clear that increasing the hygiene and sanitation level on a set of values ($\varepsilon = 0.3, 0.6, 0.9$). The results show an increase of hygiene and sanitation levels leads to a gradual reduction in individuals infected with the drug-sensitive strain of *H. pylori* bacteria. This effectively reduces transmission of H. pylori and enhances control of drug-sensitive H. pylori in the entire community.

Figure 3(b) examines the impact of varying parameter (ε) on a set of values ($\varepsilon = 0.3, 0.6, 0.9$) of individuals infected with drug-resistant *H. pylori* with time under different levels of hygiene and sanitation. The results show that increasing hygiene and sanitation levels significantly reduces and controls drug-resistant *H. pylori* infections over time in the community.

Figure 3(c) illustrates the effect of varying parameter (ε) on a set of values ($\varepsilon = 0.3, 0.6, 0.9$) of individuals infected with stomach ulcers with time under different levels of hygiene and sanitation. The infection of stomach ulcers in individuals contributed due persisted infection caused by a drug-resistant strain of *H. pylori* from the three trajectories, it is evident that poor hygiene levels at $\varepsilon = 0.3$ produce the highest peak and sustained stomach ulcer burden, while moderate hygiene $\varepsilon = 0.6$ yields an intermediate reduction. Enhanced hygiene and sanitation at $\varepsilon = 0.9$ significantly reduce the infections and minimize long-term prevalence. These results underscore the critical role of improved hygiene and sanitation in reducing stomach ulcer complications associated with drug-resistant *H. pylori* infections in the community.

Figure 3(d) examines effects of varying hygiene and sanitation levels (ε) on environmental concentration of *H. pylori bacteria* with time on progressive set values ($\varepsilon = 0.3, 0.6, 0.9$).

In all the trajectories, the bacteria concentration shows a sharp initial decline, followed by a more gradual decrease as time progresses. Higher hygiene and sanitation effectiveness $\varepsilon = 0.9$ results in a consistently lower bacterial burden and faster reduction compared to moderate $\varepsilon = 0.6$ and low $\varepsilon = 0.3$ hygiene conditions. These results demonstrates that the use of improved hygiene and sanitation plays a critical role in accelerating the reduction of H. pylori concentration and limiting its long-term environmental survival.

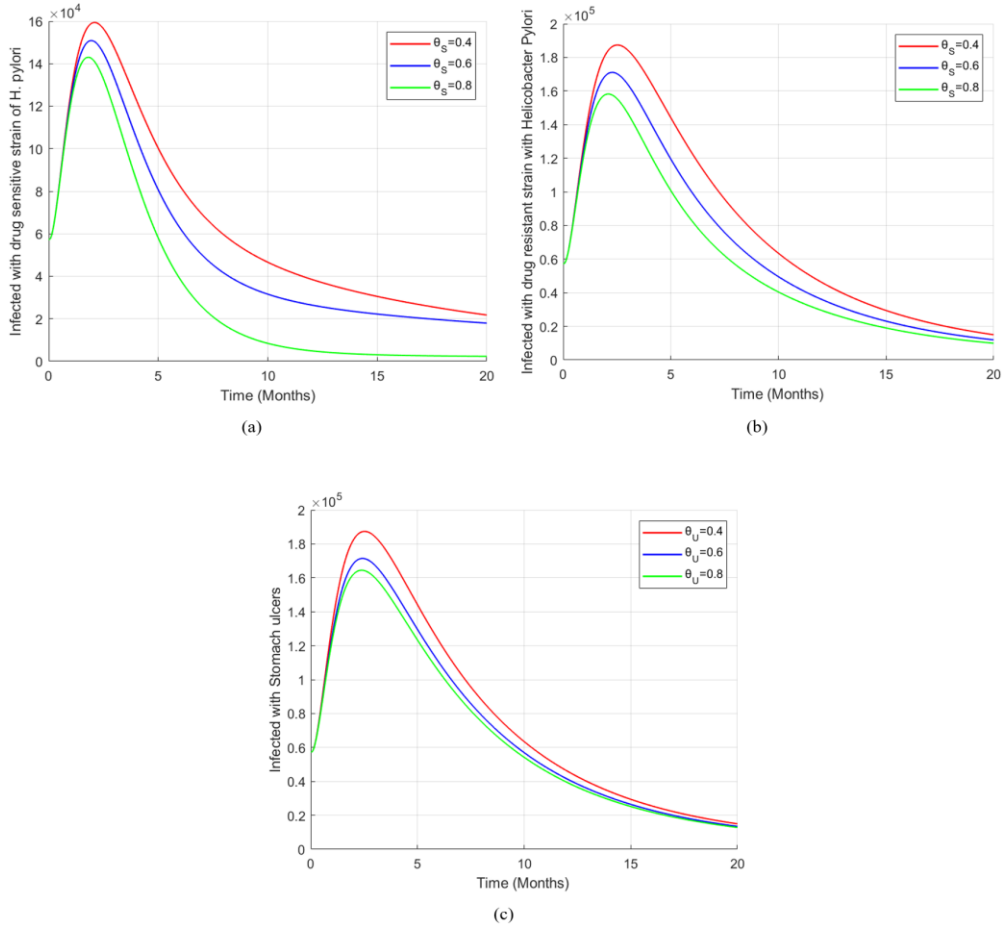

Figure 4. *Shows the effects of varying the parameter* (θ_s) *on the population trajectories of individuals with drug-sensitive and drug-resistant infections, presented in graph (a) and (b), respectively. Graph (c) shows the population trajectory of individuals with stomach ulcers when the parameter* (θ_U) *is varied.*

Figure 4(a) illustrates the effect of varying treatment efficacy(θ_s) on a progressive set of ($\theta_s = 0.4, 0.6, 0.8$) individuals infected with drug-sensitive *H. pylori* over time. The results show that an increase in θ_s indicates more effective use of first-line antibiotic treatment, which can reduce the duration of infectiousness and lower the transmission potential of the sensitive strain. However, a decrease in θ_s would result in longer infectious periods and higher transmission rates, increasing the burden of the infection. High treatment level at $\theta_s = 0.8$ leads to the quickest reduction and the lowest long-term infection level in the community. This demonstrates that increasing treatment using the first-line dose of antibiotics accelerates the control of drug-sensitive *H. pylori* infections and reduces the infection burden in the community.

Figure 4(b) illustrates the effect of varying treatment efficacy(θ_s) on progressive set ($\theta_s = 0.4, 0.6, 0.8$) individuals infected with drug-resistant H. pylori over time. The results indicate that increasing θ_s reveals more effective use of first-line antibiotic treatment, which decreases the infectious period and reduces the transmission potential of the resistant strain. Conversely, a decrease in θ_s leads to longer infectious periods and higher transmission rates, thereby increasing the disease burden. When the antibiotics used in the first-line antibiotic regimen fail, *second-line* treatment is applied. If the *H. pylori* bacteria causing the infection are resistant to *first-line* antibiotics, those drugs become less effective or ineffective in eliminating the infection. In such cases, second-line antibiotic treatments are administered, which are usually stronger and designed to treat resistant strains. This demonstrates that second-line antibiotic treatment is more effective and helps reduce both the magnitude and persistence of drug-resistant *H. pylori*. Therefore, improving treatment effectiveness can significantly suppress resistant infections in the community.

Figure 4(c) illustrates the effect of varying treatment efficacy parameter (θ_U) on a progressive set of ($\theta_U = 0.4, 0.6, 0.8$) on individuals infected with stomach ulcers with time. In all the trajectories, the number of infected individuals initially increases, and when it reaches the peak, it then declines as treatment effects take hold. It is observed that higher treatment effectiveness $\theta_U = 0.8$ results in reduced prevalence and enhanced faster reduction in ulcer infections compared to lower values such as $\theta_U = 0.6$ and $\theta_U = 0.4$. This points out that increasing treatment effectiveness for individuals with stomach ulcers significantly reduces the burden and persistence of stomach ulcer infections in the community.

5. Discussion and Conclusion

H. pylori infection continues to be a major public health concern, particularly in developing regions where sanitation infrastructure is inadequate, with children, low-income communities, and densely populated areas being most prone to infection [9]. The rise of antibiotic resistance has made treatment increasingly challenging, leading to prolonged recovery, more severe complications, and facilitating wider transmission within communities. This growing resistance underscores the urgent need for improved treatment strategies and public health interventions [27].

In this study, we developed and analyzed a mathematical model to investigate the dynamic transmission of *H. pylori* that incorporates both antibiotic-sensitive and antibiotic-resistant strains, providing a detailed understanding of infection dynamics, treatment outcomes, and transmission potential. The model incorporates the progression of individuals through various stages of infection and treatment, as well as the contamination of the environment by resistant and sensitive strains of bacteria. Timely and appropriate use of *first-line* antibiotics can effectively control infection when resistance levels are low. However, when resistant strains become prevalent, *second-line* therapies are required to prevent further spread of the disease. *Second-line* antibiotics are specifically designed to treat infections that persist following the failure of *first-line* treatment. The shift from drug-resistant to drug-sensitive cases does not mean the bacteria have genetically lost their resistance. Instead, it reflects a population-level effect: treatment suppresses resistant strains, allowing existing sensitive strains to become more dominant or detectable in clinical tests [28].

Our analysis identified the basic reproduction number ($\Re_0$) as a key threshold parameter, determining the potential for outbreaks of disease. When $\Re_0 < 1$, the disease-free equilibrium is globally asymptotically stable, indicating that the infection will die out in the long run. Conversely, if $\Re_0 > 1$, the endemic equilibrium becomes stable, leading to persistent infection within the population [25]. Sensitivity analysis was performed to help identify which parameters have the greatest impact on disease dynamics and control. The results showed that first-line treatment rates for drug-sensitive patients played a crucial role in a lower prevalence of infection, while for high prevalence, *second-line* treatment was associated with a higher prevalence of infection [28].

Effective control of *H. pylori* also requires preventive measures such as observing good hygiene practices and improving sanitation, which are essential in reducing infection prevalence and limiting community transmission [3, 9]. Controlling the infection is crucial not only to prevent transmission but also to reduce severe clinical complications, including chronic gastritis and stomach ulcers. Overall, these findings underscore the need for integrated strategies combining antibiotic stewardship, routine resistance monitoring, optimized treatment protocols, and public health interventions focused on hygiene and sanitation, while guiding future research into adaptive therapies and community-level control measures to mitigate the growing burden of *H. pylori* infections The shift from drug-resistant to drug-sensitive cases does not mean the bacteria have genetically lost their resistance. Instead, it reflects a population-level effect: treatment suppresses resistant strains, allowing existing sensitive strains to become

more dominant or detectable in clinical tests [24, 26].

The results also highlight the critical role of environmental contamination in the transmission dynamics of *H. pylori* infection, suggesting that public health interventions must address both human and environmental factors to successfully eradicate the infection. Similarly, excretion rates $\phi_S, \phi_{R,}$ and ϕ_U were found to substantially influence the environmental bacterial load, further contributing to transmission. These findings highlight the importance of focusing on both human–environment interactions and effective treatment to control, especially *H. pylori,* with the challenge of antibiotic resistance.

Numerical simulations further demonstrated the potential impact of various control strategies, including improving treatment efficacy and reducing environmental contamination. These insights can inform public health policies and strategies to reduce the burden of *H. pylori*, particularly in regions with high rates of antibiotic resistance [27]. The limitations of this study, which could be addressed in future research, include applying a stochastic approach to investigate the impact of randomness on the transmission dynamics of the diseases considered; utilizing a fractional-order model to enhance the accuracy of the results; and employing artificial intelligence techniques to improve the detection of infected individuals within the population.

Abbreviations

H. pylori	Helicobacter Pylori
DFE	Disease-Free Equilibrium
S(t)	Susceptible Individuals
I_S(t)	Individuals Infected with a Drug-sensitive Strain of H. Pylori
I_R(t)	Individuals Infected with a Drug-resistant Strain of H. Pylori
U(t)	Individuals Infected with Stomach Ulcers
R(t)	Recovered Individuals
D_H(t)	Concentration of H. pylori Bacteria in the Environment
rRNA	Ribosomal Ribonucleic Acid

Author Contributions

Vincent Kyunguti Mwanthi: Conceptualization, Data curation, Formal Analysis, Investigation, Methodology, Software, Validation, Visualization, Writing – original draft, Writing – review & editing

Stephen Karanja: Formal Analysis, Investigation, Supervision, Validation, Writing – review & editing

Loyford Njagi: Data curation, Formal Analysis, Supervision, Writing – review & editing

Mark Kimathi: Data curation, Formal Analysis, Investigation, Project administration, Supervision, Validation, Writing – review & editing

Data Availability Statement

The data used to support the findings of this study are included in the article.

Conflicts of Interest

The authors declare that there are no conflicts of interest regarding the publication of this paper.

References

[1] Savoldi, A., Carrara, E., Graham, D. Y., & Conti, M. (2020). Prevalence of antibiotic resistance in Helicobacter pylori: A systematic review and meta-analysis in different world regions. Frontiers in Microbiology, 11, 1–17. https://doi.org/10.1053/j.gastro.2018.07.007

[2] Zhang, Y., Li, J., & Chen, H. (2024). Machine learning prediction of antibiotic resistance in Helicobacter pylori using genomic data. Frontiers in Microbiology, 15, 1481763. https://doi.org/10.3389/fmicb.2024.1481763

[3] Smith, S., Fowora, M., & Pellicano, R. (2019). Infections with Helicobacter pylori and challenges encountered in Africa. World Journal of Gastroenterology, 25(25), 3183–3195. https://doi.org/10.3748/wjg.v25.i25.3183

[4] Wang, Y. (2015). Diagnosis of Helicobacter pylori infection: Current options and developments. World Journal of Gastroenterology, 21(40), 11221–11235. https://doi.org/10.3748/wjg.v21.i40.11221

[5] Amiri, M., Fard, A., & Hosseini, S. (2025). Mechanisms of antibiotic resistance in Helicobacter pylori and clinical implications. Gut Pathogens, 17(1), 1–12. https://doi.org/10.1186/s13099-025-00704-5

[6] Edelstein, Z. R., Czinn, S. J., & Blaser, M. J. (2000). A dynamic transmission model for Helicobacter pylori in the United States. Emerging Infectious Diseases, 6(3), 283–290. https://wwwnc.cdc.gov/eid/article/6/3/00-0302_article

[7] Liu, H., Li, Y., & Wang, X. (2020). A within-host model of sensitive and resistant Helicobacter pylori strains under antibiotic therapy. Journal of Theoretical Biology, 491, 110178. https://doi.org/10.1016/j.jtbi.2020.110178

[8] Malfertheiner, P., Megraud, F., O'Morain, C. A., Gisbert, J. P., Kuipers, E. J., Axon, A. T., & Graham, D. Y. (2021). Primary and secondary clarithromycin resistance in Helicobacter pylori: Implications for therapy and modeling. Nature Communications, 12(1), 1–12. https://doi.org/10.1038/s41467-021-22557-7

[9] Mutua, K. G., Ngari, C. G., Muthuri, G. G., & Kitavi, D. M. (2022). Mathematical modeling and simulation of Helicobacter pylori treatment and transmission implications on stomach cancer dynamics. Communications in Mathematical Biology and Neuroscience, 2022, Article-ID. https://doi.org/10.28919/cmbn/7314

[10] Smith, D. L., Dushoff, J., Perencevich, E. N., Harris, A. D., & Levin, S. A. (2019). Relevance of mathematical models of antimicrobial resistance in population health: Lessons from other pathogens. BMC Medicine, 17(1), 1–12. https://doi.org/10.1186/s12916-019-1314-9

[11] Malfertheiner, P., Megraud, F., Rokkas, T., Gisbert, J. P., Liou, J. M., Schulz, C., Gasbarrini, A., Hunt, R. H., Leja, M., O'Morain, C., Rugge, M., Selgrad, M., Suerbaum, S., Sugano, K., El-Omar, E. M., & European Helicobacter and Microbiota Study Group. (2022). Management of Helicobacter pylori infection: The Maastricht VI/Florence consensus report. Gut, 71(9), 1724–1762. https://doi.org/10.1136/gutjnl-2022-327745

[12] Sugano, K., Tack, J., Kuipers, E. J., Graham, D. Y., El-Omar, E. M., Miura, S., Haruma, K., Asaka, M., Uemura, N., & Malfertheiner, P. (2015). Kyoto global consensus report on Helicobacter pylori gastritis. Gut, 64(9), 1353–1367. https://doi.org/10.1136/gutjnl-2015-309252

[13] Rupnow, M. F. T., Shachter, R. D., Owens, D. K., & Parsonnet, J. (2000). A dynamic transmission model for predicting trends in Helicobacter pylori infection and associated diseases in the United States. Emerging Infectious Diseases, 6(3), 228–237. https://doi.org/10.3201/eid0603.000304

[14] Kirschner, D. E., & Blaser, M. J. (1995). The dynamics of Helicobacter pylori infection of the human stomach. Journal of Theoretical Biology, 176(2), 281–290. https://doi.org/10.1006/jtbi.1995.0198

[15] Malfertheiner, P., Camargo, M. C., El Omar, E., Liou, J. M., Peek, R., Schulz, C., & Suerbaum, S. (2023). Helicobacter pylori infection. Nature Reviews Disease Primers, 9, 20. https://doi.org/10.1038/s41572-023-00434-5

[16] Delamater, P. L., Street, E. J., Leslie, T. F., Yang, Y. T., & Jacobsen, K. H. (2019). Understanding the basic reproduction number (R_0): Calculation, applications, and limitations in epidemiology. American Journal of Public Health, 109(10), 1398–1402. https://doi.org/10.2105/AJPH.2019.305328

[17] Driessche, K., Khajanchi, S., & Kar, T. K. (2020). Transmission dynamics of tuberculosis with multiple reinfections. Chaos, Solitons & Fractals, 130, 109450. https://doi.org/10.1016/j.chaos.2019.109450

[18] Castillo-Chavez, C., Feng, Z., & Huang, W. (2002). On the computation of the basic reproduction number and its role in global stability. In Mathematical Approaches for Emerging and Reemerging Infectious Diseases (Vol. 1, pp. 229–254). Springer. https://doi.org/10.1007/978-1-4757-3667-0_13

[19] LaSalle, J. P. (1976). The stability of dynamical systems. SIAM, Philadelphia. https://doi.org/10.1137/1.9781611970432

[20] Ghotaslou, R., Leylabadlo, H. E., & Asl, Y. M. (2015). Prevalence of antibiotic resistance in Helicobacter pylori: A recent literature review. World Journal of Methodology, 5(3), 164–174. https://doi.org/10.5662/wjm.v5.i3.164

[21] Wang, J., Xie, X., Zhong, Z., Yuan, H., Xu, P., Gao, H., & Lai, Y. (2022). Prevalence of antibiotic resistance of Helicobacter pylori isolates in Shanghai, China. American Journal of Translational Research, 14(11), 7831–7841.

[22] Kirimi, E. M., Muthuri, G. G., Ngari, C. G., & Karanja, S. (2024). Modeling the effects of vaccine efficacy and rate of vaccination on the transmission of pulmonary tuberculosis. *Informatics in Medicine Unlocked, 46*, 101470. https://doi.org/10.1016/j.imu.2024.101470

[23] Tilahun, G. T., Makinde, O. D., & Malonza, D. (2017). Modelling and optimal control of typhoid fever disease with cost-effective strategies. *Computational and Mathematical Methods in Medicine, 2017*, Article 2324518. https://doi.org/10.1155/2017/2324518

[24] Oguntolu, F. A., Peter, O. J., Yusuf, A., Omede, B. I., Bolarin, G., & Ayoola, T. A. (2023). Mathematical model and analysis of the soil-transmitted helminth infections with optimal control. *Modeling Earth Systems and Environment, 9*, 355–372. https://doi.org/10.1007/s40808-022-01472-8

[25] Matsebula, L. M., Mushanyu, J., Shikongo, A., & Nuugulu, S. M. (2024). A mathematical model of cholera–typhoid coinfection dynamics with dual-seasonally driven contact rates. *International Journal of Nonlinear Sciences and Numerical Simulation*. https://doi.org/10.1515/ijnsns-2024

[26] Semeya, A. A., Abdel Hafez, R. S. A., Al-Mihy, N. F., Elgamal, R., & Othman, A. A. A. (2025). Vonoprazan-based triple therapy for *Helicobacter pylori* resistant to first-line regimens: A guideline-compliant 14-day multicenter study in Egypt. *Journal of Infection and Public Health, 18*(1), 102345. https://doi.org/10.1016/j.jiph.2024.102345

[27] Nichol, D., Jeavons, P., Fletcher, A. G., Bonomo, R. A., & Maini, P. K. (2022). *The competition dynamics of resistant and sensitive infections*. *Results in Physics*, *31*, 105181. https://doi.org/10.1016/j.rinp.2022.105181

[28] Davies, N. G., Flasche, S., & Jit, M. (2019). *Within-host dynamics shape antibiotic resistance in commensal bacteria*. *Nature Ecology & Evolution*, *3*(3), 440–449. https://doi.org/10.1038/s41559-019-0812-4